Impact of Geomagnetic Disturbances on Power System Transient Stability

Yiqiu Zhang, *Student Member, IEEE,* Komal S Shetye, *Senior Member, IEEE,*
Raymund H Lee, *Student Member, IEEE,* and Thomas J Overbye, *Fellow, IEEE*
Department of Electrical and Computer Engineering
Texas A&M University
College Station, TX, USA
{yzhang458, shetye, lee32982, overbye}@tamu.edu

***Abstract*—Geomagnetic disturbances (GMDs) can potentially impose operational challenges on power systems and cause damage to essential grid assets through geomagnetically induced currents (GICs). The impacts of GICs on steady state voltage stability are now well-known. However, less is known about the impacts of GICs on power system transient stability, especially in the presence of contingencies. Using different metrics, this paper investigates the impacts of GMDs on power system transient stability by applying different single element contingencies to a 10k-bus synthetic network in the presence of time-invariant GMDs. Several case studies are presented as examples of the potential effects of GMDs. The results show that GMDs can alter power system transient margin. Therefore, relevant transient stability studies may need to be conducted to ensure secure power system operations under the effect of GMDs.**

Keywords—Geomagnetic disturbances (GMDs), geomagnetically induced currents (GICs), single element contingency, power system transient stability.

I. Introduction

Geomagnetic disturbances (GMDs) due to solar coronal mass ejections (CME) have the potentials for causing great difficulties on grid operations and damage to grid assets [1]-[2]. When a CME reaches the Earth, charged particles injected into the earth's magnetosphere will induce quasi-dc electric fields with frequencies ranging from 0.01 Hz to 0.5 Hz at ground level. As a result, geomagnetically induced currents (GICs) will be induced on transmission lines [3]-[6]. GICs tend to cause half-cycle saturation in high-voltage transformers, which causes the transformers to absorb more reactive power and experience more harmonic currents [2]-[3], [6]-[8]. In these situations, power systems are more likely to encounter the damage of transformers or a voltage collapse [9].

Using a 10k-bus synthetic network [10]-[12], this paper examines the impacts of GMDs on the power system transient stability after the occurrence of different single element contingencies. Previous works such as [13] and [14] investigated the transient voltage stability of small systems under the effect of GMDs. Reference [13] examined how the ramping rates of electric fields, load models, and voltage controls influence the voltage stability. Reference [14] studied how different characteristics of electric fields impact the transient voltage stability during a high altitude electromagnetic pulse (HEMP), a special GMD event as the result of nuclear explosion. Both of the papers used GMDs as the disturbances to the systems, with the severity levels of the disturbances dependent on the characteristics of the electric fields such as rise time, decay time, and duration. Instead, this paper uses the typical single element contingencies as the disturbances and assumes a constant electric field throughout each simulation. The assumption of a constant electric field is justified by the fact that naturally-occurring GMDs, usually with frequencies much below 1 Hz, do not vary much during the transient time frame of several dozen seconds. Moreover, both the voltage stability and rotor angle stability [15] of the 10k-bus system are evaluated using different metrics (e.g. maximum voltage drop and critical clearing time).

This paper is organized as follows. Section II includes an overview of the GIC modeling in transient stability analysis. Section III presents the transient stability case studies where different single element contingencies are applied to the system in the presence of time-invariant GMDs. Section IV concludes the paper.

II. Overview of GIC Modeling in Transient Stability Analysis

A. GIC Modeling in Transient Stability

This section gives an overview of how GICs are modeled in transient stability analysis in [14]. GICs induced on transmission lines impact power systems by causing half-cycle saturation of transformers and in turn increasing the reactive power losses in the transformers. For each of the transformers, the reactive power loss due to GICs can be determined by solving

$$Q_{Loss,pu} = V_{pu} K I_{GIC,pu} \quad (1)$$

where $Q_{Loss,pu}$ is the reactive power loss; V_{pu} is the ac voltage of the transformer's high-side terminal bus; K is a constant which maps the GICs to the losses and depends on the characteristics of the transformer; $I_{GIC,pu}$ is an adjusted version of the GIC where the transformer parameters are incorporated [16]-[18]. All the variables with the subscript "pu" are expressed in per unit. GICs participate in the dynamics of the system as additional constant current reactive loads and alter the reactive power balance equations of the transient stability model [14] as follows.

978-1-5386-7138-2/18/$31.00 ©2018 IEEE

$$Q_{Gen,i} - Q_{L,i} - Q_{Loss,i} - \sum_{k=1}^{n} V_i V_k Y_{ik} \sin(\theta_i - \theta_k - \alpha_{ik}) = 0, \quad i = 1, \ldots, m \tag{2}$$

$$- Q_{L,i} - Q_{Loss,i} - \sum_{k=1}^{n} V_i V_k Y_{ik} \sin(\theta_i - \theta_k - \alpha_{ik}) = 0, \quad i = m+1, \ldots, n \tag{3}$$

Equation (2) and equation (3) show the reactive power balance at a generator bus and a load bus, respectively. The system has n buses in total, m among which are the generator buses. The reactive power consumed by a load at bus i is represented as $Q_{L,i}$. At a high-side terminal bus i of a transformer, the reactive power loss due to GIC is represented as $Q_{Loss,i}$. At a generator bus i, the reactive power supplied by a generator is represented by $Q_{Gen,i}$. V and θ are the bus voltage and bus angle with the subscript (i, k) showing the bus number. The admittance between bus i and bus k and associated angle are given by Y_{ik} and α_{ik}, respectively [14]. With combination of a set of differential equations and other constraints [19], the system states can be determined using numerical integration. Equation (1) will be performed at each iteration to update $Q_{Loss,i}$ in (2) and (3).

III. GMD Transient Stability Case Studies

A. Contingencies and Synthetic Network in Use

1) Single Element Contingencies in Use

Generator outage, transformer outage, and temporary short-circuit of a transmission line are the three single element contingencies used in this paper. Each of the contingencies is repetitively applied to the system in the absence of a GMD or in the presence of electric fields with different magnitudes. The detailed descriptions of the contingencies are available in their corresponding sections.

2) 10k-bus Test System

A 10k-bus synthetic electric grid [10]-[12] is used for the transient stability studies in this paper. The 10k-bus synthetic network is a fictitious system, which mimics the actual power system on the footprint shown in Fig.1, and does not contain any critical electric infrastructure information (CEII). Equipped with dynamic models and geographic coordinates, the synthetic network can be used for transient stability analysis with the effects of GICs taken into consideration.

B. Voltage Transient Stability Analysis for a Generator Outage

In the presence of a time-invariant and uniform electric field, the voltage transient stability of the system is examined following the loss of one of the biggest generators in Arizona. The electric field has a direction of 77 degrees, with north as the reference (0 degrees). A 77-degree electric field is chosen, because it will result in the maximum reactive power loss for the system. The electric field is increased from 0 to 7 V/km (The power flow does not converge beyond 7 V/km.) in steps of 1V/km. 0 V/km electric field is equivalent to "in the absence of a GMD". Under the electric field, the generator is opened at the first second and the next nineteen seconds of voltage response is recorded for a bus in Arizona and a bus in Oregon,

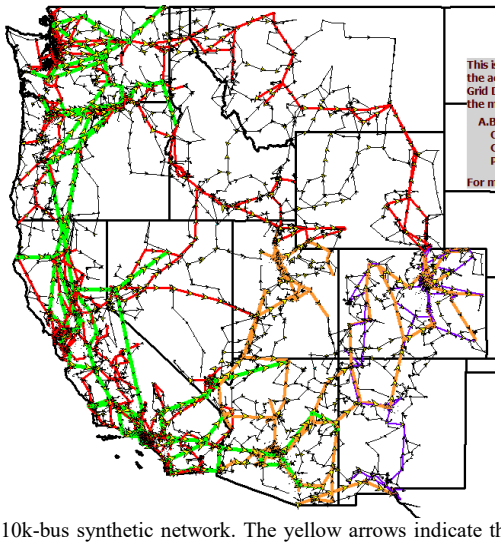

Fig.1. 10k-bus synthetic network. The yellow arrows indicate the flow of GICs under a 1V/km uniform electric field at 77 degrees with north as the reference (0 degrees).

respectively. These buses are selected for their relatively large variations in their maximum voltage drops under the effect of GMDs.

1) Description of the Opened Generator

The opened generator in Arizona is connected to a high voltage bus (765 kV) though a generator step-up (GSU) transformer. Under normal conditions (i.e. in the absence of a GMD), the generator provides 1397.5 MW, and is at its maximum Mvar output limit of 516.4, with its maximum MW output limit to be 1403.2 MW.

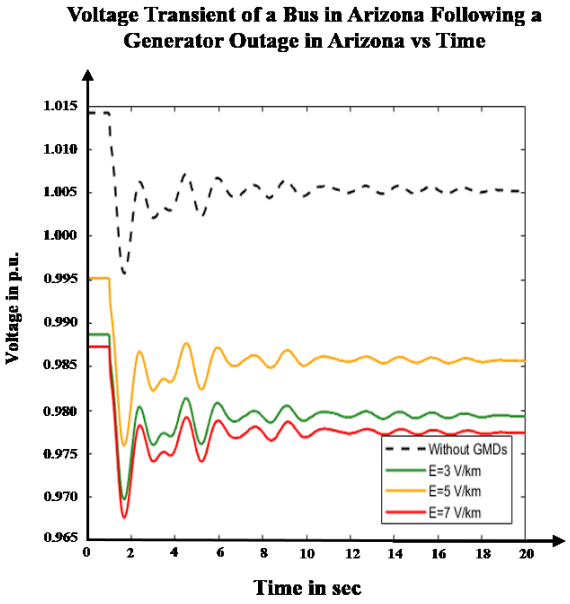

Fig.2. The actual pre-contingency voltage values and voltage variations of a bus in Arizona after the occurrence of the generator outage in Arizona under the effect of different GMDs.

2) Metric in Use: Maximum Voltage Drop

The maximum voltage drop after the occurrence of the contingency is used as the metric in this section. The maximum voltage drop is defined as the difference between the initial voltage and the lowest voltage following the contingency.

3) Voltage Transient of the Monitored Bus in Arizona

The impact of the GMDs on the voltage transient stability of a bus in Arizona is evaluated. The bus of interest is the high-side terminal bus of a 500kV-115kV transformer. Fig.2 shows the actual initial voltage values in the first second (before the occurrence of the contingency) and voltage variations for the next nineteen seconds of the bus. The curves in different colors represent the voltages of the same bus, with the system subjected to the 77-degree electric fields with different magnitudes (i.e. 0, 3, 5, and 7 V/km), respectively. Since power flow solutions determine the initial voltages prior to the contingency and the electric field magnitudes determine the reactive power losses due to GICs, the initial voltage of the bus in Arizona is observed to vary with different electric field magnitudes. However, the initial voltage is not positively correlated to the electric field magnitude, given that the yellow curve (E = 5 V/km) is above the green curve (E = 3 V/km) in Fig.2. This observation is caused by the inclusion of shunt switching in the power flow. In the presence of the 5 V/km electric field, discrete capacitor switching near the bus in Arizona is observed, which explains why the initial voltage under this condition is greater than that under a lower electric field level.

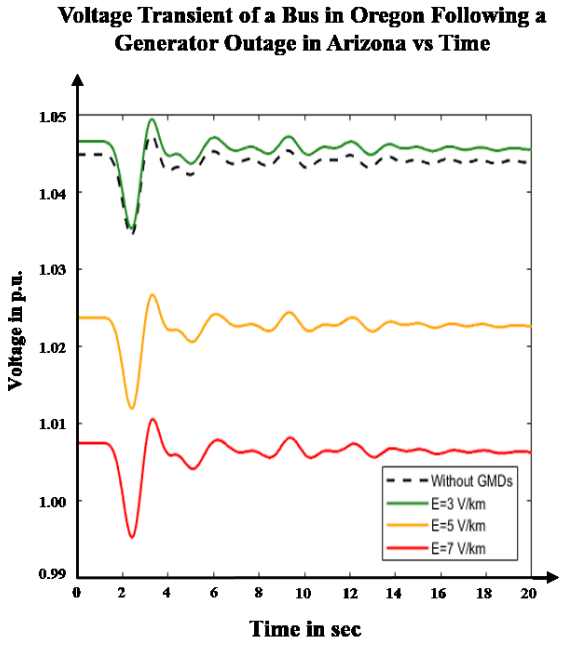

Fig.3. The actual pre-contingency voltage values and voltage variations of a bus in Oregon after the occurrence of the generator outage in Arizona under the effect of different GMDs.

4) Voltage Transient of the Monitored Bus in Oregon

Following the generator outage, the voltage response of a bus in Oregon is also recorded and shown in Fig.3, which is organized the same way as Fig.2. The bus of interest is the high-side terminal bus of a 765kV-345kV transformer and connected to four small generators, through GSU transformers. The same set of observations made from Fig.2 can also be made from Fig.3. Under the effect of GMDs, changes in voltage dynamics, reflected by changes in the maximum voltage drop, are also observed and shown in Table I and Table II for the bus in Arizona and the bus in Oregon, respectively.

TABLE I
VOLTAGE VARIATION SUMMARY OF THE BUS IN ARIZONA UNDER DIFFERENT ELECTRIC FIELDS

Electric Field Magnitude (V/km)	Initial Voltage (p.u.)	Maximum Voltage Drop (p.u.)	Lowest Voltage (p.u.)
0	1.0142	0.0185	0.9957
3	0.9887	0.019	0.9697
5	0.9952	0.0193	0.9759
7	0.9873	0.0197	0.9676

TABLE II
VOLTAGE VARIATION SUMMARY OF THE BUS IN OREGON UNDER DIFFERENT ELECTRIC FIELDS

Electric Field Magnitude (V/km)	Initial Voltage (p.u.)	Maximum Voltage Drop (p.u.)	Lowest Voltage (p.u.)
0	1.0448	0.0108	1.0340
3	1.0465	0.0115	1.0350
5	1.0237	0.0117	1.0120
7	1.0075	0.0122	0.9953

Table I and Table II show the actual initial voltages, maximum voltage drops, and actual lowest voltages for the bus in Arizona and the bus in Oregon under the effect of the different electric fields, respectively. It is observed that the initial voltage variations of either bus are on the order of 0.01 p.u., while the variations in the maximum voltage drop for either bus are on the order of 0.001 p.u. Therefore, the variations of the lowest voltage are more dependent on the changes in the initial voltage than on the dynamics. Moreover, there is a positive correlation between the maximum voltage drop and electric field magnitude observed in Table I and Table II, which suggests that GICs may tend to negatively impact the voltage transient stability of the system. Given the monitored buses' distances from the contingency, GICs can not only impact the voltage transient of the buses near the contingency, but also those of the buses far from the contingency.

C. Rotor Angle Transient Stability Analysis for a Transformer Outage

In this section, the rotor angle transient stability of the system is examined following the loss of an EHV transformer in Arizona. The rotor angle transient of a generator in Arizona is monitored in the absence of a GMD or in the presence of a 77-degree uniform electric field (with north as 0 degrees) of 1 V/km or of 2 V/km. Since the generator experiences an unacceptable increment and instability in its rotor angle under the 1 V/km electric field and 2 V/km electric field, respectively, the usage of a metric becomes unnecessary in this case.

1) Description of the Opened Transformer

A 500kV-115kV Wye-Wye autotransformer with both its windings grounded is opened at the first second in Arizona. Under the electric field of 1 V/km, the reactive power absorbed by the transformer is 35.36 Mvar. With the magnitude of the electric field increasing to 2 V/km, the reactive power absorption increases to 70.71 Mvar. Since the reactive power loss imposed on the transformer due to GICs is modeled as a constant current reactive load,

the system will experience a sudden reactive load loss upon the transformer outage.

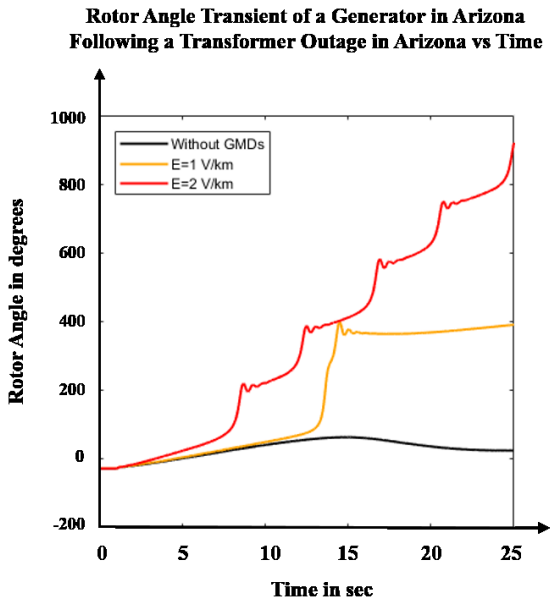

Fig.4. An EHV transformer in Arizona is opened at t = 1 sec. The rotor angle of a generator at a substation, named NOGALES, in Arizona is monitored in the absence or presence of GMDs.

2) Description of the Monitored Generator

The generator of interest is located at a substation, named NOGALES, in Arizona and connected with the high-side terminal bus of a 500kV-115kV wye-wye grounded autotransformer through a GSU transformer. The generator can provide a maximum of 27 MW and 13.743 Mvar. The substation containing the opened transformer is connected with substation NOGALES by a 500kV 77km long transmission line. The machine, exciter, governor, and stabilizer models of the monitored generator are GENROU, EXPIC1, GGOV1, and IEEEST, respectively [20].

3) Rotor Angle Transient of the Monitored Generator

The rotor angle of the monitored generator in Arizona in the absence or presence of a GMD is presented in Fig.4. Fig.4 shows the pre-contingency rotor angle in the first second and the rotor angle transient for the next twenty four seconds following the transformer outage. In the absence of a GMD, the rotor angle increases from -27 to 63.7 degrees and eventually reaches an equilibrium rotor angle of 37.6 degrees. In the presence of the 77-degree electric field of 1 V/km, the rotor angle of the generator experiences a maximum of 425.7-degree increment, settling at 405.9 degrees. However, such a significant change in a generator rotor angle is prohibited in actual power system operations, since the change can cause an unacceptable power swing and make the system less secure. Practically, a generator experiencing a significant change in its rotor angle will be disconnected from the system by out-of-step protective relays to prevent equipment damage, and other system effects. The red curve in Fig.4 indicates that the rotor angle of the generator becomes unstable under the effect of the 77-degree electric field of 2 V/km.

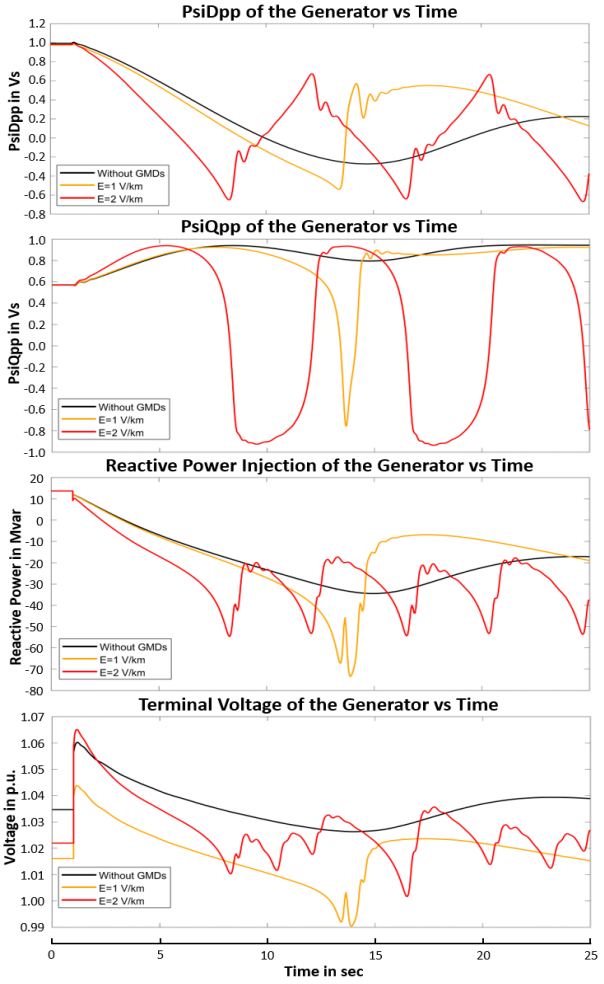

Fig.5. State variable variations of the monitored generator in the absence of a GMD or in the presence of different GMDs.

Fig.5 provides the transients of different state variables of the monitored generator. The first two subplots show flux linkage variations (i.e. PsiDpp and PsiQpp) of the generator, while the third and fourth subplots show the Mvar injection and terminal voltage magnitude, respectively. The black, yellow, and red lines in each subplot show the variations of the state variable at E = 0 V/km (in the absence of a GMD), E = 1 V/km, and E = 2 V/km, respectively. Upon the transformer outage (at t = 1 sec), the terminal voltage of the generator spikes as the result of a sudden increase in Mvar flow into substation NOGALES. The generator reduces its Mvar injection into the network and even starts to absorb Mvar out of the network, as the Mvar flow into substation NOGALES gradually increases. The above description and explanation apply to all three GMD scenarios considered here. At E = 1 V/km, the rate of change of the Mvar flowing into substation NOGALES starts to increase around t = 12 sec until the valve opening/closing rate limit of the generator's governor is violated around t = 13.5 sec. This violation may trigger a control action which causes the reactive power injection to change from decreasing to increasing and stabilizes the generator's rotor angle around t = 13.5 sec, as shown in Fig.4. At E = 2 V/km, the same limit violation occurs around t = 8.3 sec. The same reasoning can also be used to explain why the red line in the third subplot changes from decreasing to increasing at that time.

Average Bus Frequency Responses at Substations in the Presence of Different Electric Fields

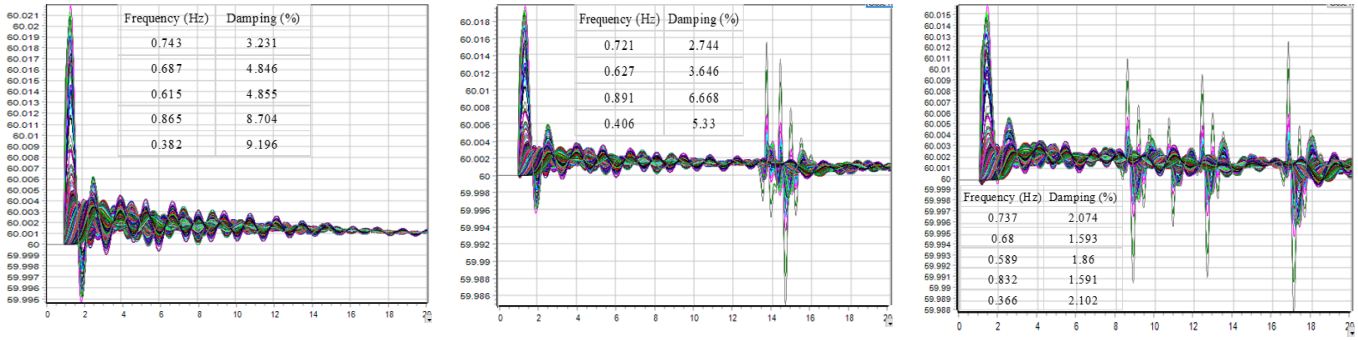

(a) E=0 V/km **(b) E=1 V/km** **(c) E=2 V/km**

Fig.6. An EHV transformer in Arizona is opened at t =1 sec. The average of bus frequencies at each substation is shown for different electric fields.

This case suggests that GMDs can potentially cause rotor angle instability through a relatively low electric field. During a severe GMD event, GICs will substantially increase and saturate transformers, especially EHV and UHV transformers. The transformers can be permanently damaged from overheating. The outage of the transformers in such an event will result in more serious consequences, given that the system is burdened with a high reactive power demand and faced with a large disturbance caused by the sudden loss of a significant amount of reactive load.

4) Modal Analysis of Frequency Results during Transformer Outage

Fig.4 shows the rotor angle of a single generator under different GMD conditions. We now look at bus frequency results of the same set of simulations, such as those that may be recorded by devices such as PMUs, to assess the system wide effects. The average of bus frequencies at each substation is the selected signal in this analysis.

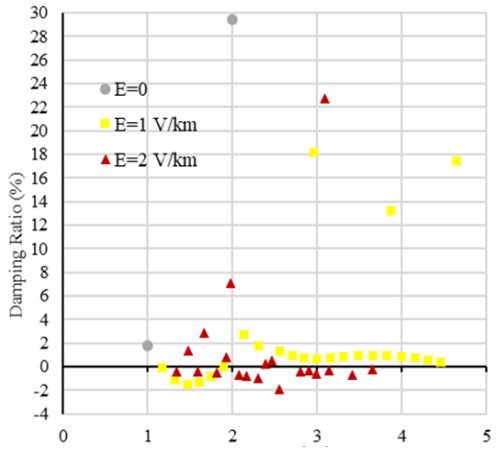

Fig.7. Modes of oscillation versus their damping ratios where the largest weighted percentage signal is from substation NOGALES

In the absence of a GMD, both Fig.4 and Fig.6 (a) indicate that the system is stable. Fig.6 (b) shows the sudden commencement of an oscillation observed at several buses at around t = 13 sec, which coincides with the onset of the instability from the rotor angle results in Fig.4. Similarly, Fig.6 (c) shows oscillations earlier, at around t = 9 sec. There is a certain periodicity in these results (i.e. t = 9, 13, 17 and so), which match up with the times when the "notches" occur in the red curve in Fig.4. Fig.6 also shows the key modes with low damping ratios (i.e. < 10%) for each scenario. The damping of these modes reduces progressively as the applied electric field increases. Moreover, the electric field introduces instabilities, by causing negatively damped oscillations most from one particular generating substation named NOGALES. These are shown in Fig.7.

D. Rotor Angle Transient Stability Analysis for a Temporary Balanced Three-Phase Line Fault

In this section, the rotor angle transient stability of the system is examined following a balanced three-phase fault on a line in Utah. Through the observation of the first occurrence of rotor angle instability, the critical clearing time (CCT) of the fault is determined under the effect of an electric field at 77 degrees, with north as the reference. The magnitude of the electric field varies from 0 to 4 V/km in steps of 1 V/km. 0 V/km electric field is equivalent to "in the absence of a GMD".

TABLE III
CCTs UNDER THE EFFECT OF DIFFERENT ELECTRIC FIELDS

Electric Field Magnitude (V/km)	Critical Clearing Time (s)
0	0.427
1	0.421
2	0.419
3	0.411
4	0.404

1) Metric in Use: Critical Clearing Time (CCT)

CCT is a commonly used metric for evaluating the transient stability of a system after the occurrence of short-circuit faults [21]. CCT is defined as the maximum duration for which a short-circuit fault can last without the system losing its synchronism [21]. This section determines the CCT by gradually increasing the fault duration in the steps of 0.001s and using the time just before the observation of the first unstable rotor angle of a generator.

2) Description of the Faulted Transmission Line

A balanced three-phase fault is applied to a 56.8 km long 500kV transmission line in Utah. The substations connected by the line have no generators.

3) CCTs Under the Effect of Different GMDs

In the absence of a GMD or in the presence of the individual 77-degree electric field with different magnitudes, the critical clearing time of the fault is determined. Table III shows that CCT decreases as the electric field magnitude increases. Moreover, it is observed that the rotor angle of the generator nearest to the faulted line always becomes unstable first under the different electric fields. This observation can be explained by the fact that generators, especially the ones close to the contingency, are more stressed due to increased reactive power demand under the effect of increased GICs. In this specific case, the CCTs in the presence of GMDs are shorter than that in the absence of a GMD. As the result of a decreased CCT, the circuit breakers designed for normal conditions (in the absence of a GMD) may not be able to react promptly in the presence of GMDs. Equipment damage and service interruption are more likely to occur in this situation.

IV. Conclusion

This paper investigated the impacts of GMDs on power system transient stability following different single element contingencies, by performing case studies on a 10k-bus synthetic network. Both the voltage stability and rotor angle stability were evaluated using the maximum voltage drop and critical clearing time as the metrics, respectively. The results of the case studies suggest that power system transient margin can be altered by the presence of GMDs. After the occurrence of a generator outage, the maximum voltage drops of a bus near the generator and a bus far from the generator were observed to vary positively with the electric field magnitude. Moreover, GICs due to a relatively low electric field were observed to be detrimental to the rotor angle transient stability and synchronism of certain generators following the loss of an element such as a transformer. Also, the rotor angle dynamics evaluated with the critical clearing time of a balanced three-phase fault are altered under the effect of different GMDs. The key takeaway is that in addition to steady state power flow studies for voltage stability assessments, transient stability studies may also need to be conducted to adequately plan and prepare for operating grids securely in the presence of GMDs.

Acknowledgment

This work was supported by NSF under Award number EAR-1520864, and by Bonneville Power Administration through the Technology Innovation Project #359 titled “Improved System Modeling for GMD and EMP Assessments”.

References

[1] W. A. Radasky, "Overview of the impact of intense geomagnetic storms on the U.S. high voltage power grid," *2011 IEEE International Symposium on Electromagnetic Compatibility*, Long Beach, CA, USA, 2011, pp. 300-305.

[2] V. D. Albertson, J. M. Thorson, R. E. Clayton and S. C. Tripathy, "Solar-Induced-Currents in Power Systems: Cause and Effects," in *IEEE Transactions on Power Apparatus and Systems*, vol. PAS-92, no. 2, pp. 471-477, March 1973.

[3] IEEE Guide for Establishing Power Transformer Capability while under Geomagnetic Disturbances - Corrigendum 1," in *IEEE Std C57.163-2015/Cor 1-2016 (Corrigendum to IEEE Std C57.163-2015)*, vol., no., pp.1-11, Jan. 12 2017.

[4] T. J. Overbye, K. S. Shetye, T. R. Hutchins, Q. Qiu and J. D. Weber, "Power Grid Sensitivity Analysis of Geomagnetically Induced Currents," in *IEEE Transactions on Power Systems*, vol. 28, no. 4, pp. 4821-4828, Nov. 2013.

[5] J. G. Kappenman, W. A. Radasky, J. L. Gilbert and L. A. Erinmez, "Advanced geomagnetic storm forecasting: a risk management tool for electric power system operations," in *IEEE Transactions on Plasma Science*, vol. 28, no. 6, pp. 2114-2121, Dec 2000.

[6] V. D. Albertson, J. G. Kappenman, N. Mohan and G. A. Skarbakka, "Load-Flow Studies in the Presence of Geomagnetically-Induced Currents," in *IEEE Transactions on Power Apparatus and Systems*, vol. PAS-100, no. 2, pp. 594-607, Feb. 1981.

[7] D. H. Boteler and E. Bradley, "On the Interaction of Power Transformers and Geomagnetically Induced Currents," in *IEEE Transactions on Power Delivery*, vol. 31, no. 5, pp. 2188-2195, Oct. 2016.

[8] M. Lu, H. Nagarajan, E. Yamangil, R. Bent, S. Backhaus and A. Barnes, "Optimal Transmission Line Switching Under Geomagnetic Disturbances," in *IEEE Transactions on Power Systems*, vol. 33, no. 3, pp. 2539-2550, May 2018.

[9] "2012 Special Reliability Assessment Interim Report: Effects of Geomagnetic Disturbances on the Bulk Power System, " NERC, Feburary. 2012. [Online]. Available: https://www.eenews.net/assets/2012/02/29/document_pm_01.pdf

[10] A. B. Birchfield, T. Xu, K. M. Gegner, K. S. Shetye and T. J. Overbye, "Grid Structural Characteristics as Validation Criteria for Synthetic Networks," in *IEEE Transactions on Power Systems*, vol. 32, no. 4, pp. 3258-3265, July 2017.

[11] Electric Grid Test Case Repository (2017). [Online]. Available: https://electricgrids.engr.tamu.edu/electric-grid-test-cases/activsg10k/.

[12] T. Xu; A. B. Birchfield; K. S. Shetye; T. J. Overbye,“Creation of synthetic electric grid models for transient stability studies,” accepted by 2017 IREP Symposium Bulk Power System Dynamics and Control, Espinho, Portugal, 2017.

[13] T. J. Overbye, K. S. Shetye, Y. Z. Hughes and J. D. Weber, "Preliminary consideration of voltage stability impacts of geomagnetically induced currents," *2013 IEEE Power & Energy Society General Meeting*, Vancouver, BC, 2013, pp. 1-5.

[14] T. R. Hutchins and T. J. Overbye, “Power system dynamic performance during the late-time (E3) high-altitude electromagnetic pulse,” in *Power Systems Computation Conference (PSCC)*, 2016. IEEE, 2016, pp. 1-6.

[15] IEEE/CIGRE joint task force on stability terms and definition," definations and classifications of power system stability," IEEE Trans. Power Systems, vol. 19, no. 2.pp. 1387-1401, 2004.

[16] K. Zheng, "Effects of system characteristics on geomagnetically induced currents", *IEEE Trans. Power Del.*, vol. 29, no. 2, pp. 890-898, Sep. 2013.

[17] T. J. Overbye, T. R. Hutchins, K. Shetye, J. Weber, S. Dahman, "Integration of geomagnetic disturbance modeling into the power flow: A methodology for large-scale system studies", Proc. 2012 North American Power Symp., 2012-Sep.

[18] H. Zhu, T. J. Overbye, "Blocking Device Placement for Mitigating the Effects of Geomagnetically Induced Currents", IEEE Trans. Power Systems, vol. 30, no. 4, pp. 2081-2089, Jul. 2015.

[19] P. W. Sauer and M. A. Pai, Power System Dynamics and Stability, Champaign, IL: Stripes Publishing LLC, 1997.

[20] [Online]. Available: https://www.powerworld.com/WebHelp/Content/TransientModels_HTML/Generator.htm?tocpath=Transient%20Stability%20Add-On%20(TS)%7CTransient%20Models%7CGenerator%7C____0/.

[21] L. G. W. Roberts, A. R. Champneys, K. R. W. Bell, M. di Bernardo, "Analytical approximations of critical clearing time for parametric analysis of power system transient stability", *IEEE J. Emerging Sel. Topics Circuits Syst.*, vol. 5, no. 3, pp. 465-476, Sep. 2015.